Learning from Sensors and Past Experience in an Autonomous Oceanographic Probe

Albert Vilamala, Enric Plaza, Josep Lluis Arcos

IIIA, Artificial Intelligence Research Institute
CSIC, Spanish National Research Council
Campus UAB, E-08193, Bellaterra, Spain
{vilamala, enric, arcos}@iiia.csic.es

Abstract

The work presented in this paper is part of a multidisciplinary team collaborating in the deployment of an autonomous oceanographic probe with the task of exploring marine regions and take phytoplankton samples for their subsequent analysis in a laboratory. We will describe an autonomous system that, from sensor data, is able to characterize phytoplankton structures. Because the system has to work inboard, a main goal of our approach is to dramatically reduce the dimensionality of the problem. Specifically, our development uses two AI techniques, namely Particle Swarm Optimization and Case-Based Reasoning. We report results of experiments performed with simulated environments.

Introduction

Recent advances in optical and acoustical instrumentation have allowed the study of ocean water constituents such as phytoplankton dynamics in a way not feasible some years ago. Specifically, the current research on underwater optical properties can be used to characterize from large scale marine patterns to small scale events.

The work presented in this paper is part of a multidisciplinary effort where oceanographic biologists, mechanical and electronic engineers, and computer scientists are collaborating in the deployment of an autonomous oceanographic probe able to explore marine regions and gather water samples interesting for their phytoplankton structure. These phytoplankton structures are known as *Thin Layers* (Dekshenieks et al. 2001; Stramska and Stramski 2005).

Different biological studies have proved that thin layers have an important impact on the biological structure and dynamics of marine systems. Nevertheless, because the composition and location of the thin layers vary with the time and they are small structures (their range in thickness is from few centimeters to a few meters), their study and localization is still an open research topic.

The goal of the project is to develop new autonomous sampling instruments to help oceanographic biologists to understand the distribution and composition of thin layers in different oceanographic regions. The application scenario is
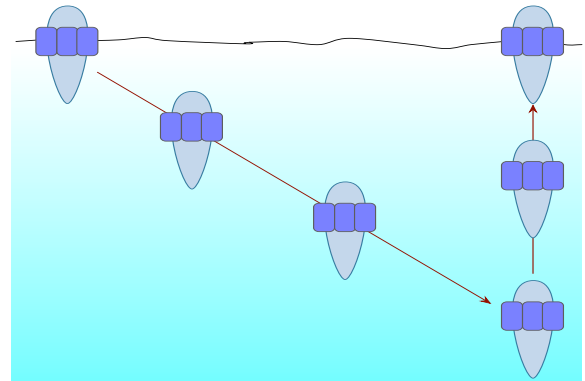
Figure 1: Diagram of the probe's trajectory.

an autonomous probe continuously descending and ascending in a given oceanographic region for analyzing the possible presence and composition of thin layers and gathering some water samples. During descent (from the surface to a given depth) the probe uses its sensors to capture data on the presence of organic matter in suspension. Analysis of these data inboard the probe detects the most likely distribution of thin layers. Since the probe's descent disturbs the thin layers by its passing through, this descent is made in a diagonal trajectory from surface to the established depth, at which point the probe ascends in a vertical trajectory, as shown in Fig. 1. The ascension is now on undisturbed thin layers, and during this trajectory the probe will use its water bottles to obtain samples at the depths in which these layers are predicted to be according to the analysis of the sensor data. There are two main issues to solve here: (1) determining the number, depth and shape of thin layers, and (2) given the limited number of water bottles (around 10) to obtain samples, deciding the moments in which water bottles should be closed to obtain samples. The method to map the action of closing N bottles and the depth levels at which these bottles will take samples is not part of the identification component presented here.

This paper describes how two different Artificial Intelligence techniques have been combined to design an identification component able to determine when water samples have to be gathered. The identification component addresses two different tasks: the detection of thin layers from several
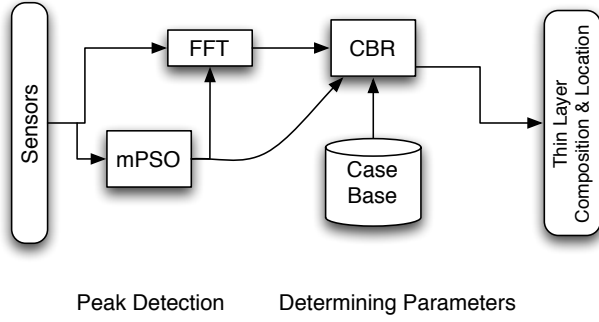
Figure 2: Diagram of the component's architecture.

data streams (coming from inboard optical sensors continuously measuring); and the characterization of their composition and location. The first task is accomplished with a swarm approach whereas the second task is performed by a case-based reasoning module.

The paper is organized as follows: the next section describes the task performed by the AI component and details the design of two different AI modules; then we empirically evaluate the performance of the identification component by using 300 simulated environments and, finally, we draw some conclusions and discuss the future research lines.

The identification component

The identification component addresses two different issues: the detection of possible thin layers and the characterization of these thin layers. Regarding the first issue, spectral downwelling irradiance distributions (E_d) obtained by hyperspectral sensors are used to detect thin layers. From E_d, the following four parameters that characterize a thin layer can be calculated: the main algae group, the thickness, the concentration, and the depth. Specifically, concentration is estimated by the attenuation coefficient K_d in a depth z for a given wavelength λ as follows:

$$K_d(z, \lambda) = -\frac{ln[E_d(z_2, \lambda)/E_d(z_1, \lambda)]}{z_2 - z_1} \quad (1)$$

where z_1, z_2 are the previous and subsequent depths to the target z where E_d was measured.

Applying the previous formula we may determine the possible presence of thin layers by looking for irradiance peaks. In the design of the identification component we used 300 simulations generated by the experts using the Hydrolight-Ecolight 5.0 numerical model (Mobley and Sundman 2008). Each simulation provides the measurements of the downwelling irradiance with a depth resolution of $5cm$ and a spectral resolution of $1nm$ for a given marine scenario. Specifically, we work with scenarios where two different thin layers (varying in depth, thickness, and concentration) are present.

Nevertheless, the sensors provide a huge amount of data, and only a low consuming algorithm is feasible. Thus, we decided to use a *multi Particle Swarm Optimization* (mPSO)

algorithm to detect irradiance peaks. mPSO is an optimization technique based on the movements of a collection of particles that are selectively sampling a complex function landscape (Poli, Kennedy, and Blackwell 2007).

Moreover, each algae group has specific characteristics that produce different irradiance responses. This diversity of response requires a two-step approach, where first main algae type has to be identified and only then the other parameters may be precisely determined. Thus, a wrong identification of the algae group may produce a higher error in determining the other parameters. The current simulations cover four different types of algae families.

We have designed a Case-Based Reasoning (CBR) module for the characterization of the thin layers. CBR is an AI technology that directly reasons from previous experiences (Leake 1996). In our domain this feature is interesting because the nature of the domain knowledge is empirical, and a theoretical biological model is not yet available. Moreover, because CBR is a technology where reasoning and learning are intimately connected, it facilitates future steps of the project.

The mPSO module

Particle Swarm Optimization (PSO) aims at producing a collaborative intelligent behavior based on the metaphor of social interaction (Kennedy and Eberhart 1995). The movements of each particle are based on combining a cognitive model with a social model. The cognitive model drives each particle to its best position so far. The social model drives each particle to the best position found by particles in its neighborhood.

In PSO, each particle has a position $\vec{p}_i$ and a velocity $\vec{v}_i$. Initially, the set of particles is randomly distributed with a random initial velocity in the search space, which is a 2-dimensional matrix (depth × frequency). The position and velocity of each particle is modified iteratively: after a particle moves, the sensor value associated to the current particle's position is read. The two equations that govern the movements of each particle are the following:

$$\vec{v}_i = \chi(\vec{v}_i + \vec{U}(0, \phi_1)(\vec{b}_i - \vec{p}_i) + \vec{U}(0, \phi_2)(\vec{g} - \vec{p}_i)) \quad (2)$$

$$\vec{p}_i = \vec{p}_i + \vec{v}_i \quad (3)$$

where χ is the constant multiplier that ensures the convergence; $\vec{p}_i$ is the current position of the particle i; $\vec{v}_i$ is the velocity of the particle i; $\vec{b}_i$ the best position found by the particle i; $\vec{g}$ the global best solution found by the particles; and $\vec{U}(0, \phi_i)$ represents a vector of random numbers uniformly distributed in $[0, \phi_i]$.

Since 2001, when Eberhart and Shi proposed the original PSO for solving dynamic optimization problems, different authors have proposed extensions to the original PSO algorithm, such as resetting the particles position frequently or using a multi-swarm model (Poli, Kennedy, and Blackwell 2007) for improving its adaptiveness in dynamic environments (Blackwell 2007). In our project we have used a multi-swarm approach inspired on the mQSOE model
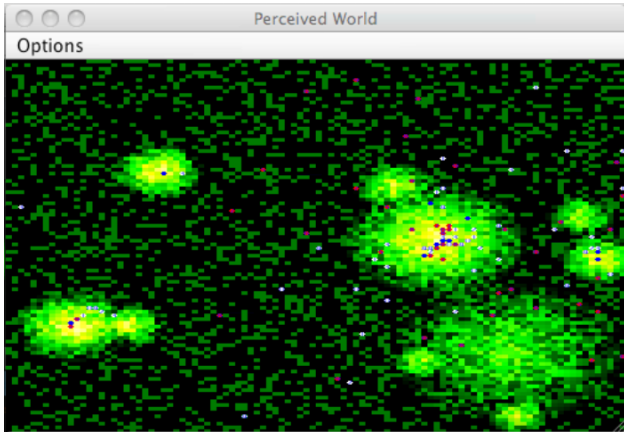
Figure 3: The mPSO algorithm working in a noisy environment.

(Fernandez-Marquez and Arcos 2009). The multi-swarm approach is appropriate in multi-modal problems (i.e. when several peaks appear at the same time). However, simply dividing a global swarm into a set of independent swarms does not guarantee success. At least a new operator has to be introduced: the *exclusion* operator.

Exclusion operator: The exclusion operator is introduced to ensure that two sub-swarms are not exploiting the same peak, i.e. to guarantee *swarm diversity*. Two sub-swarms are considered to be close to each other when their attractors (best solutions) are within an exclusion radius. When this occurs, the sub-swarm with a lower solution is reinitialized in the search space.

Launching swarms: Each time the probe completes a descendant path, the peaks detection algorithm is fired. The peaks detection algorithm uses 4 swarms of 10 particles to explore a given simulation (the measurements of a specific marine scenario). The standard PSO parameters have been set following (Blackwell 2007), while the swarm exclusion radius was set following (Blackwell and Branke 2005). We only allow the access to 10^4 measures (i.e. each particle performs only 250 movements). Figure 3 shows an example of a multi swarm exploring a multi peak environment. Notice that the irregularity in the environment is generated by the presence of noise affecting the measurements.

The output of mPSO is a set of detected thin layers expressed as pairs composed of depth and K_d (estimated concentration).

The CBR module

Case-Based Reasoning (Kolodner 1993) is an AI approach that capitalizes on previous problem-solving experiences when solving new problems, retrieving similar past cases and reusing their solutions to determine the predicted solution for a new problem; see (Mantaras et al. 2005) for an overview on CBR. This section presents the CBR model of the probe indentification of thin layers: we will define what a *case* is in the domain of thin layers (*Case definition*), how

similar cases are retrieved (*Retrieve process*), and how the retrieved cases are used to predict the solution of a new situation (*Reuse process*).

The inputs for the CBR component are the sensor data and the output from mPSO. Preliminary experiments showed that only using concentration peaks, as detected in the previous section, was not enough: we need to take into account both *peaks and contour*. For this purpose, we determine the Discrete Fourier Transform (DFT) (Agrawal, Faloutsos, and Swami 1993) of the sensor data, and select the first 4 coefficients as a higher-level representation of the thin layer contour.

Case definition: A case is represented as pair $\langle P, S \rangle$ where P is a problem description and S a solution description. In the thin layers domain a problem description is a tuple $P = \langle f_1, f_2, f_3, f_4, K_d, \omega \rangle$, where $f_1, \ldots, f_4$ are the first 4 coefficients of the DFT applied to the sensor data, K_d is the attenuation coefficient (estimating concentration), and ω is the *full width at half maximum*[1] of a normal distribution (estimating thickness). A solution is described by a tuple $S = \langle \alpha, \theta, \eta \rangle$, where the three parameters are the algae type (α), the (real) thickness (θ) and the (real) concentration (η). Thus, when a new problem is addressed by the CBR module, the problem's sensor data is transformed to DFT and the first 4 coefficients obtained define the *new case* $\langle P', S' \rangle$. The outcome of the CBR module for a new problem P' is a prediction of a new solution S', namely algae type, thickness and concentration of the thin layer described by P'.

Retrieve: The Retrieve process of CBR estimates the similarity of the new problem with those present in the case base, in our module using an Euclidean distance over the $f_1, \ldots, f_4$ coefficients. Since a coefficient is a complex number ($f_j = r_j + ic_j$), the Euclidean distance is computed over 8 dimensions ($r_1, \ldots, r_4, c_1, \ldots, c_4$). A number k of more similar cases is the output of the Retrieve process. Different experiments were performed to elucidate the value of k, which was set (for the results reported here) to $k = 3$.

Reuse: The Reuse process builds a *local model* based on the nearest cases (the k retrieved cases) and applies it to predict the solution of the new case. Specifically, the Reuse has to determine the solution tuple $\langle \alpha', \theta', \eta' \rangle$ (i.e. algae type, thickness and concentration) of the new case based on the solutions (i.e. tuples $\langle \alpha, \theta, \eta \rangle$) of the retrieved cases. Algae type α is determined by majority vote of the algae types in the retrieved cases.

In order to predict the numerical values of the (real) thickness (θ) and the (real) concentration (η) we cannot directly use the estimation of the input data (K_d and ω respectively). For that purpose, we use the case base a second time, now

---

[1]The full width at half maximum (FWHM) is an estimation of the extent of a function such as duration of a pulse in a waveform. Specifically, FWHM is the difference between the two extreme values of the independent variable at which the dependent variable is equal to half of its maximum value. Assuming that thin layer concentration has a normal distribution, FWHM can be computed from the standard deviation.
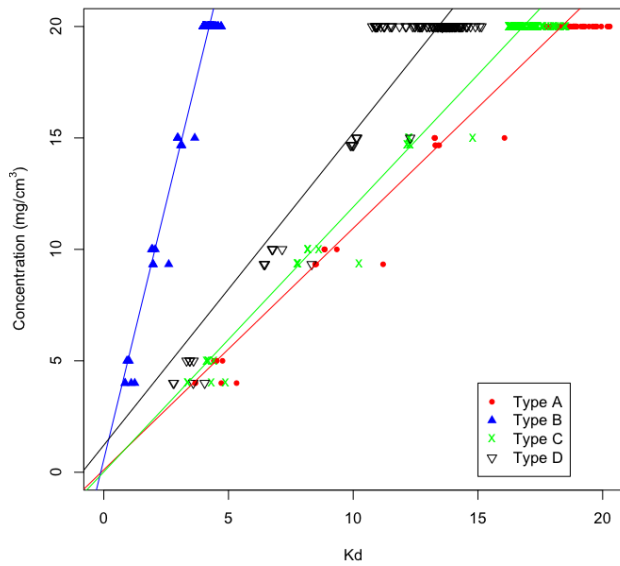
Figure 4: Linear regression models (for each algae type) between estimated concentration (K_d) and real concentration (η).

Figure 5: Linear regression models (for each algae type) between estimated thickness (ω) and real thickness (θ).

to determine how estimators K_d and ω diverge from the real values θ and η in each of the known cases. Moreover, since this divergence may depend on the algae type, we use a linear regression method to find the multiplicative factor that relates estimated values to real values for each algae type. Figure 4 shows the linear regression model relating estimated concentration (K_d) with the real concentration (η) for the 4 algae types (each one represented as a different line). The predicted value for real concentration (η) is determined using the linear regression model of algae type α at the value K_d.

Similarly, Figure 5 shows the linear regression model relating estimated thickness (ω) with the real thickness (θ) for the 4 algae types; the figure shows that the linear regression model for thickness is much less dependent on algae type than before. The predicted value for real thickness (θ) is determined using the linear regression model of algae type α at the value ω.

In summary, the CBR module outputs the solution $S' = \langle \alpha', \theta', \eta' \rangle$ for a problem P' by predicting the algae class α' of the most similar cases and predicting thickness θ' and concentration η' by a regression-based adaptation of the estimators of thickness and concentration in the input of the current problem.

Experiments

The goal of the experiments was to validate the accuracy and robustness of the identification component. Two different sets of experiments were designed to test separately the peak detection module and the case-based reasoning module.

For testing our system, we have used 300 water column scenarios generated by the experts using the Hydrolight numerical model. Hydrolight (Mobley and Sundman 2008) is
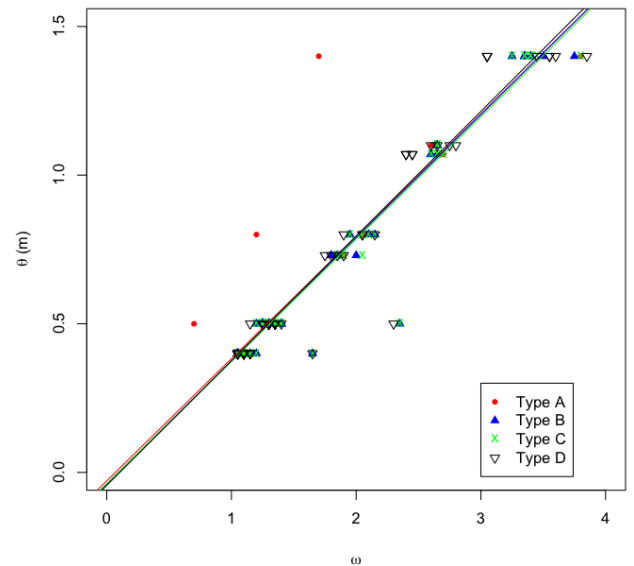
a radiative transfer numerical model that computes spectral radiance distributions and related quantities for water bodies. A scenario consists of measurements of the attenuation coefficient (K_d) from 0 to 15 meters depth (with a sample at each $5cm$) and ranging from $400nm$ to $650nm$ (with a spectral resolution of $1nm$). Each scenario has two thin layers at different depths (i.e. we have models of 600 thin layers). The thin layers present in a simulation vary in depth (from $4m$ to $12m$), thickness (from $0.4m$ to $1.4m$), and concentration (from $4mg/m^3$ to $20mg/m^3$). Finally, we applied different noise levels to the input signals in order to test the robustness of our approach.

Thin layers detection

We used 40 particles grouped in 4 different swarms, i.e. each swarm with 10 particles. Our method required accessing just 13% of the 7.5×10^4 measurements existing for each model. The results presented below are the average of 20 runs per scenario.

Because each simulation contains two different thin layers, the difficulty of detecting both thin layers depends on their proximity and on their size difference. A detailed analysis of the experiments revealed that the proximity factor (with a minimum value of 3.5 meters) does not increase the average error. On the other hand, the hardest problems are those where the first thin layer presents a high concentration and the second layer presents a low concentration. In these simulations some of the runs were not able to detect the second thin layer (see 1st row in Table 1).

For the simulations where the thin layer is detected, the 2nd row in Table 1 shows the peak depth error in centimeters. First, notice that the level of error in thin layer detection is independent of the depth. Moreover, the experiments show that the error is smaller than the depth resolution ($5cm$). Finally, the algorithm detection of thin layers' depth

Noise	0 %	10 %	20 %	30 %	40 %	50 %
Failures	1.38	1.62	1.64	1.67	1.75	1.82
Error	2.8	3.3	3.4	3.9	4.1	4.2
Std.Dev.	3.0	6.0	7.4	8.3	9.8	10.8

Table 1: Peak detection failures (%), error (cm), and standard deviation, given noise levels ranging from 0% to 50%.
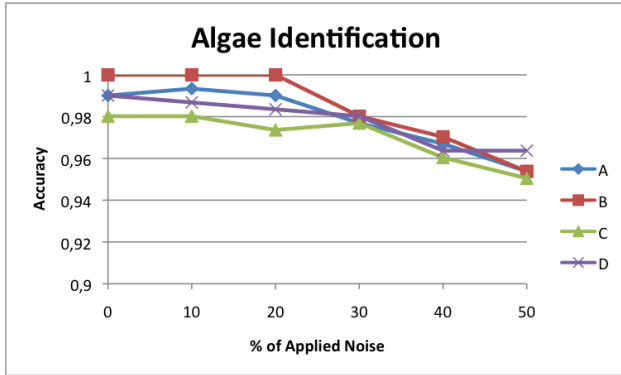

Figure 6: Accuracy in algae identification when applying noise levels ranging from 0% to 50%.

is robust in the presence of noise, since both failure rate and error are not degraded excessively with a noise up to 50%.

Characterizing thin layers

This subsection presents an experimental evaluation of thin layers characterization performed by the CBR module. For this purpose, as before, we strain the CBR module by applying noise levels ranging from 0% to 50%.

The first task of the CBR module is to identify the main algae type in a thin layer. We asses the CBR module's accuracy by a set of experiments performing 10-fold cross-validation. Before applying noise to the data, Figure 6 shows that accuracy is between 98% and 100% depending on the algae type. Applying noise up to 30% the identification accuracy is not degraded significantly (see Figure 6). Notice that the accuracy of algae type B is kept at 100% up to a noise level of 20%. At noise levels higher than 30%, although the performance declines, accuracy is still around 95% at 50% of noise.

Table 2 summarizes the precision, sensitivity, and specificity of the CBR module with a noise level of 30% (the noise cut level). Although there are differences on these measures depending on the algae type, they are not statistically significant. Finally, Table 3 shows the accuracy of the CBR module in predicting concentration and thickness in the scenario without noise for the 4 algae types. Since the error is less than 5%, the identification is robust enough for an autonomous probe.

Conclusions and future work

We have presented the design and development of an autonomous system that determines the depth and features of

Algae Types	A	B	C	D
Precision	0.97	0.96	0.95	0.93
Sensitivity	0.93	0.96	0.94	0.98
Specificity	0.99	0.98	0.98	0.97
Accuracy	0.97	0.98	0.97	0.98

Table 2: Algae identification analysis with a 30% of noise.

Algae Types	A	B	C	D
Concentration	0.95	0.97	0.96	0.97
Thickness	0.96	0.97	0.96	0.97

Table 3: Concentration and thickness accuracy on the 4 algae types.

phytoplanktonic thin layers given the input captured by the oceanographic probe sensors. Our development uses two AI techniques, namely Particle Swarm Optimization and Case-Based Reasoning. A major issue in developing a system that works upon sensor data is to dramatically reduce the dimensionality of the problem. Sensor data of one problem is, in our domain, a matrix with 75,000 elements, where every element is a floating point number. The mPSO module samples about a 10% of the matrix data, already achieving a large reduction. The mPSO output is a vector of radiance values at 250 frequencies, achieving a second large dimensionality reduction.

Since only using concentration peaks was not sufficient, we needed to capture information about the contour of the thin layers. The DFT operation effectively captures this information, and allows another large dimensionality reduction by selecting only the first 4 coefficients. The CBR module is then able to work with a highly compact and efficient case representation, where the problem is described by 10 dimensions: the Fourier coefficients' 4 complex numbers, the attenuation coefficient, and the FWHM width.

Although our experiments are based on synthetic data, the case-base and the sensor data are based on commercial simulators and have been generated by experts from the Marine Technology Unit (UTM-CSIC). The experiments show that the accuracy of the system is high, and thus we expect that it would constitute an adequate identification module for the probe when deployed in the second half of 2010. Notice that the probe, by design, needs to have a robust decision system from the start — engineering it from synthetic but reasonably accurate data was a necessity.

We plan to acquire real data from the deployment of the oceanographic probe, on top of which we can apply the same methodology and obtain a second, more adapted, decision module for an autonomous probe. Undoubtedly real data may present new challenges to address, but our current work has shown the feasibility of using these or other AI techniques in this problem domain.

The final decision of when to take samples (i.e. closing the water bottles in the probe) remains future work. These decisions are a direct consequence of the number of bottles, the number of detected thin layers, and the characterization
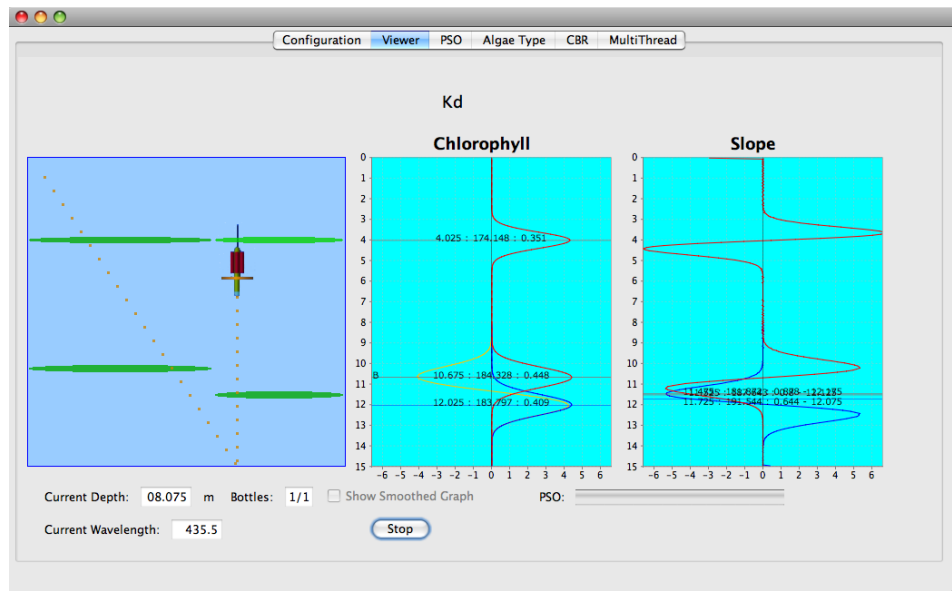
Figure 7: Snapshot of the Simulator Framework.

of these thin layers in terms of algae type, depth, concentration and thickness. In our planned approach, the probe will include a set of expert-defined rules that perform this mapping, implementing (1) default strategies (e.g. one sample at each thin layer's concentration peak) and (2) immersion-specific tactical decisions (e.g. the biologist may indicate preference of information sampling for specific algae types). Immersion-specific tactical decisions are needed to override defaults, and ensure the capability of the probe to perform repeated immersions in the same area and acquire several different collections of samples. Ensuring this variety of samples is critical for oceanographic probes.

Acknowledgments

References

Agrawal, R.; Faloutsos, C.; and Swami, A. 1993. Efficient similarity search in sequence databases. In *Foundations of Data Organization and Algorithms*, volume 730 of *Lecture Notes in Computer Science*. Springer Verlag. 69–84.

Blackwell, T., and Branke, J. 2005. Multiswarm, exclusion, and anti-convergence in dynamic environments. *IEEE Trans. Evolutionary Computation* 10(4):459–472.

Blackwell, T. 2007. Particle swarm optimization in dynamic environments. In Yang, S.; Ong, Y.-S.; and Jin, Y., eds., *Evolutionary Computation in Dynamic and Uncertain Environments*, volume 51 of *Studies in Computational Intelligence*. Springer. 29–49.

Dekshenieks, M.; Donaghey, P.; Sullivan, J.; Rines, J.; Osborn, T.; and Twardowski, M. 2001. Temporal and spatial occurrence of thin phytoplankton layers in relation to physical processes. *Marine Ecology Progress Series* 223:61–71.

Fernandez-Marquez, J., and Arcos, J. 2009. An evaporation mechanism for dynamic and noisy multimodal optimization. In *Proceedings of the 10th Genetic and Evolutionary Computation Conference (GECCO'09)*, 17–24.

Kennedy, J., and Eberhart, R. C. 1995. Particle swarm optimization. In *Proc. of the IEEE international conference on neural networks IV*, 1942–1948.

Kolodner, J. 1993. *Case-based Reasoning*. Morgan Kaufmann.

Leake, D. B., ed. 1996. *Case-Based Reasoning: Experiences, Lessons and Future Directions*. MIT Press.

Mantaras, R.; McSherry, D.; Bridge, D.; Leake, D.; Smyth, B.; Craw, S.; Faltings, B.; Maher, M.; Cox, M.; Forbus, K.; Keane, M.; Aamodt, A.; and Watson, I. 2005. Retrieval, reuse, revision, and retention in CBR. *Knowledge Engineering Review* 20(3):215–240.

Mobley, C. D., and Sundman, L. K. 2008. Hydrolight-ecolight 5.0 user's guide. Technical report, Sequoia Scientific, Inc., Bellevue, WA.

Poli, R.; Kennedy, J.; and Blackwell, T. 2007. Particle swarm optimization. an overview. *Swarm Intelligence* 1:33–57.

Stramska, M., and Stramski, D. 2005. Effects of a nonuniform vertical profile of chlorophyll concentration on remote-sensing reflectance of the ocean. *Applied Optics* 44:1735–1747.